Article

UAVs in Disaster Management: Application of Integrated Aerial Imagery and Convolutional Neural Network for Flood Detection

Hafiz Suliman Munawar [1] **, Fahim Ullah** [2,*] **, Siddra Qayyum** [1] **, Sara Imran Khan** [3] **and Mohammad Mojtahedi** [1]

[1]   School of Built Environment, University of New South Wales, Kensington, Sydney, NSW 2052, Australia;
       h.munawar@unsw.edu.au (H.S.M.); s.qayyum@unsw.edu.au (S.Q.); m.mojtahedi@unsw.edu.au (M.M.)
[2]   School of Civil Engineering and Surveying, University of Southern Queensland,
       Springfield, QLD 4300, Australia
[3]   Faculty of Chemical Energy, University of New South Wales, Kensington, Sydney, NSW 2052, Australia;
       saraimrankhan17@gmail.com
*   Correspondence: fahim.ullah@usq.edu.au

Abstract: Floods have been a major cause of destruction, instigating fatalities and massive damage to the infrastructure and overall economy of the affected country. Flood-related devastation results in the loss of homes, buildings, and critical infrastructure, leaving no means of communication or travel for the people stuck in such disasters. Thus, it is essential to develop systems that can detect floods in a region to provide timely aid and relief to stranded people, save their livelihoods, homes, and buildings, and protect key city infrastructure. Flood prediction and warning systems have been implemented in developed countries, but the manufacturing cost of such systems is too high for developing countries. Remote sensing, satellite imagery, global positioning system, and geographical information systems are currently used for flood detection to assess the flood-related damages. These techniques use neural networks, machine learning, or deep learning methods. However, unmanned aerial vehicles (UAVs) coupled with convolution neural networks have not been explored in these contexts to instigate a swift disaster management response to minimize damage to infrastructure. Accordingly, this paper uses UAV-based aerial imagery as a flood detection method based on Convolutional Neural Network (CNN) to extract flood-related features from the images of the disaster zone. This method is effective in assessing the damage to local infrastructures in the disaster zones. The study area is based on a flood-prone region of the Indus River in Pakistan, where both pre-and post-disaster images are collected through UAVs. For the training phase, 2150 image patches are created by resizing and cropping the source images. These patches in the training dataset train the CNN model to detect and extract the regions where a flood-related change has occurred. The model is tested against both pre-and post-disaster images to validate it, which has positive flood detection results with an accuracy of 91%. Disaster management organizations can use this model to assess the damages to critical city infrastructure and other assets worldwide to instigate proper disaster responses and minimize the damages. This can help with the smart governance of the cities where all emergent disasters are addressed promptly.

Keywords: convolutional neural network (CNN); disaster management; aerial imagery; flood detection; unmanned aerial vehicles (UAVs)

1. Introduction

Floods are characterized by an enormous water flow in large magnitudes into dry lands from water bodies such as lakes, rivers, and oceans [1]. Generally, the water level change in the water bodies is not closely monitored, especially in developing countries, and is usually neglected until it results in flood-related disasters [2]. On average, 60,000 lives are lost globally to natural disasters every year [3]. Furthermore, floods are the most frequently occurring natural disasters globally, representing 40% of the total natural disasters [4,5].

Apart from many fatalities, these floods cause huge damage to a country's economy by damaging its critical infrastructure, agricultural lands, smart real estate and other properties, as well as mobility and transportation [6–10]. For example, flood events between 2016 and 2017 impacted 85 million people, with an annual loss of approximately USD 36.7 billion [11]. In 2011, the damages to agriculture due to floods had been estimated to be more than USD 249 million in the Philippines alone [12]. These floods are responsible for a 59% loss of infrastructure and 87% loss of livestock [13]. The extent of damage can be controlled by taking appropriate steps to combat the emergencies caused by the floods. The US National Weather Service (NWS) reported deaths of 126 people and property damage worth 10 million by the 2016 floods, recording it as one of the highest death tolls caused by weather-related disasters in the US [14].

Researchers are investigating the use of advanced digital technologies to aid smart city governance, real estate, and disaster management [5,9,15–21]. One way of planning a proper disaster response is to have an external surveillance system that does not rely on local servers. An immediate response can be initiated if the flood is detected early by a sophisticated external surveillance system [22,23]. Such an external system can provide comprehensive and reliable information about the affected region to disaster management and rescue authorities [6]. A candidate approach for devising such a system is to perform flood mapping of the affected region through images captured from unmanned aerial vehicles (UAVs) using 5G or 6G communications [24–26]. This can highlight the areas affected by floods and help save people's lives, agricultural lands, real estate, infrastructure, and properties by doing timely damage assessments to plan relief activities efficiently [27,28]. Flood maps can be constructed by retrieving data from satellite imagery, UAVs, aircraft, or remote sensing (RS) techniques [18,24,25,29]. The image data captured by satellite can help perform proper risk assessments of the affected area to instigate a proper disaster response [4,5,30]. RS is a cost-effective approach as it reduces search efforts and provides immediate rescue resources [31].

Similarly, geographical information systems (GIS) are also investigated to aid the flood-related disaster management process [23,32]. According to Lyu et al. [33], flood forecasting is conducted based on four types of regional flood risk assessment methods, including (i) statistical methods, (ii) multi-criteria analysis, (iii) analysis using GIS and RS, and (iv) scenario-based analysis. Conversely, the real-time diagnosis is time-consuming and laborious, delaying the response and putting lives at risk. Image classification and segmentation techniques such as support vector machines (SVM) have also been used to evaluate the extent of the flood damage [34]. SVM supports RS when a small amount of data are used. However, when the data are complicated and involve complex operations, the results may not be ideal for planning a proper, timely disaster response. Recent complexities shifted the technology towards adopting and utilizing deep learning where different approaches, such as Deep Belief Networks (DBN) [35], Convolutional Neural Networks (CNN) [36,37], and Recurrent Neural Networks (RNN) [38,39] are employed for task recognition, object detection, and associated region classification. Among these techniques, CNN is the most widely used technology with excellent performance in most tasks, such as image classification, feature extraction, and segmentation. CNN learns features from a large database automatically through multi-layers of neurons and can implement non-linear decision functions [27,37].

Accordingly, CNN-based deep learning models have been used in the current study to detect floods from input aerial images captured through UAVs. The UAVs can also move into tight and congested places and collect pictures to provide insights into the critical infrastructure, complex buildings, and homes during flood events. The CNN-based deep learning model has been selected due to its excellent performance in image segmentation and classification tasks. Deep learning has been used in this study to highlight flooded regions in the images captured through UAVs. The aim is to support disaster management authorities to quickly map flooded regions to initiate relief and evacuation operations as soon as possible. The specific case study explored in the current study is from a developing country (Pakistan) which is a novelty of the current study. Previous studies have not

explored Pakistan for UAV-based disaster management systems. Such approaches can be adopted by countries with similar economies as well as developed countries to developing UAV-based disaster management approaches. Furthermore, the damage assessment can be conducted for critical infrastructures such as bridges, buildings, and smart grids. The main goals achieved by this research align well with the United Nations International Strategy for Disaster Reduction and Sendai Framework for Disaster Risk Reduction 2015–2030.

The rest of the paper is organized as follows: Section 2 presents the state-of-the-art methods adopted for flood prediction, detection, and mapping. Deep learning models and image processing have been studied to gain insights into the current study. Section 3 discusses the methodology followed in conducting this research. This includes selecting the study area, dataset collection, CNN architecture design, experimental setup, model training, and testing phases. Section 4 presents the experimental results where the flood detection output on input test images has been illustrated. Further Section 4 discusses the results and highlights the findings and achievements of this research, and Section 5 concludes the paper.

2. Literature Review

In recent years, various researchers and disaster planners have emphasized developing effective flood warning and forecasting systems to mitigate disasters and plan efficient responses. Table 1 presents some of the state-of-the-art methods from the past decade proposed for flood management. Artificial Neural Network (ANN) for flood prediction and forecasting has been frequently observed in the literature [40]. For example, Sankaranarayanan et al. [41] used a deep neural network for flood forecasting. The authors used weather data such as rainfall intensity and temperature to train a multilayer ANN model to warn about a possible flood event. Such models can assess the potential damages to the infrastructure as well as homes and buildings in case of heavy rainfalls. Similarly, Doubleday J [42] used multiple hidden layers instead of a single one in their ANN model that yielded much higher accuracy than a traditional ANN model. Their proposed flood plain mapping system used SVM to segment the cloud, land, and water regions from satellite imagery that achieved an overall classification accuracy of 92%. However, their study is limited due to the usage of remotely sensed images, which are prone to noise and are weather-dependent. Further, such images cannot be attained for darker spaces such as in the building basements, areas under the bridges and other concealed areas. This dependency restricts the application in instigating immediate disaster responses as clouds are usually present during rain-related floods.

Elsafi [43] utilized an ANN model to predict flood events using upstream flow data using the river Nile case study in Sudan. Using the data related to flow at the upstream locations, the flows at certain river locations were simulated using a trained ANN model to predict flood events. Anusha and Bharathi [44] studied flood detection and mapping and used image processing techniques such as thresholding to identify water regions from input images. The dataset was collected by obtaining Synthetic Aperture Radar (SAR) images of the target area. Pre-processing was done to remove speckle noise from images by applying a median filter followed by image rectification. A pixel-based threshold was subsequently applied to classify each pixel as "water" or "non-water".

Table 1. Review of Recent Flood Management Studies.

Technique Used	Focus of the Study	Advantages of the Techniques	Limitation of the Techniques
Deep Neural Network [41]	Flood Prediction	Higher accuracy than traditional ANN.	Dataset is not recent. It contains records from the year 1992 to 2002. Imbalance in data distribution was not considered.
Support Vector Machine (SVM) [42]	Flood Plain Mapping	Overall classification accuracy >90%	Presence of noisy data in the training dataset. Relatively old data (1965–2003).
Artificial Neural Network (ANN) [40,43]	Flood Prediction	Reduced analytical costs as less time are required for analyzing the data	Use of only one variable for training; suitable in situations where there is a lack of data.
Image Segmentation using Thresholding [44]	Flood Detection and Mapping	Identification of inundated areas can be used as key inputs for flood modeling and analysis.	Reduced accuracy in case of hyper-spatial data.
Random Forest and Multilayer Perceptron (MLP) Models [45]	Flood Detection & Flood Depth Modeling	Reduced expense (computation time and resources) of large-scale hydraulic models through the integration of machine learning	- Large number of trees makes the processing of the algorithm too slow. - Not practical for real-time predictions and applications.

Similarly, a study by Li et al. [46] show encouraging results where the proposed CNN framework has improved the κ statistic from 0.614 to 0.686 (7%) compared to its supervised counterpart. Improved precision for flooded open areas (FO) (from 0.506 to 0.684) is obtained at the cost of a slight decrease in recall (from 0.842 to 0.824), while both precision and recall for flooded built-up areas (FB) increase. In another study by Zhao et al. [47], CNN performed better than the SVM and random forests (RF), with an accuracy of 0.90 for CNN and 0.88 for LeNet-5 in the testing period. Similarly, Hosseiny et al. [45] used RFs for flood detection, coupled with the MLP model for flood depth detection in the target regions. The RF method yielded an accuracy of 98.5% in detecting the flooded regions and the MLP model achieved a regression coefficient of 0.88 for depth. Thus, the expense of simulations in large-scale hydraulic models can be reduced using this much simpler machine learning approach.

Other studies focused on using a warning system during flood situations and emphasized "warning communities" as a solution to overcome the disastrous effects caused by the floods [48]. Alfieri et al. [49] developed a flash flood warning system based on a probabilistic framework that uses a threshold exceedance method during heavy rainfalls. An index was also defined for measuring the severity of forecasted rainfall. Narayanan et al. [50] employed a method that measures and estimates the flood level from captured images using computer vision. These images may be captured and uploaded by the people in the disaster-hit area on the server. The authors used the Scale-invariant feature transform (SIFT) method for feature processing of the image. The geographical location of the region was acquired through geo-tagging information to plan an effective disaster response. Mousa et al. [51] used flood sensors for calculating the flood water level through ultrasonic range finder and temperature sensors.

The ANN approach was used to process the sensor's data and estimate the water level in key infrastructure, homes, and smart structures (Lin and Hu, 2018). Artificial Intelligence (AI) systems to control the disaster by mining data from social media platforms such as Facebook, Twitter, and Instagram have also been introduced and utilized by various studies [52,53]. The status updates, picture uploads, and comments have provided an emergency response with AI algorithms trained to recognize such images and comments and provide relief responses to the affected regions. For example, Facebook uses CNN for tagged face detection, and Google uses it for speech recognition and photo searching [54].

UAVs have been used and explored in many fields, such as smart real estate [9,15], smart cities [55], healthcare [56], and others. In the disaster management field, UAVs have been explored for post-disaster management using IoT [57], energy-efficient task scheduling and physiological assessment [58], public safety in disaster and crisis management [59], flood management, and others [4]. In addition, various techniques involving machine learning have been explored for efficient flood disaster management through UAVs. The specific applications include ANN, CNN, SVM, Image segmentation, and others [60–62]. The latest research focuses on CNN applications in flood disaster management using UAVs [63]. A key advantage of UAVs is their ability to move into any space and collect data, including pictures and real-time insights into the damage to the key infrastructure. UAVs have used CNN to extract images and videos to assess damages to structures, homes, and buildings induced by floods and leakages, such as pipeline leakages and real-time flood assessment [64,65]. The current study aligns with the latest research and explores CNN's applications for post-flood disaster management, devising a swift response to initiate rescue operations and assessing damages to critical infrastructure.

CNN has been used in multiple flood-related studies. In a study led by Mason et al. [66], the flood images shared on social media were fed to embedded metadata to detect flood patterns. The CNN approach was used on an already trained ImageNet to extract clear visual information from images uploaded onto social media. Word embedding was used by metadata for feeding textual information to a bi-directional RNN. Furthermore, glove vectors were used to set the word embedding, and the final images and text were combined to get an output that consisted of related information about the flood. Mar-

tino [67] developed an AI system that detected flood events from social media, retrieved them, and derived their visual properties and metadata with a multi-modal approach. The pre-processing of the images was carried out, which consisted of cropping and pre-filtering based on the color and textual metadata. Lopez-Fuentes [68] used the CNN approach with Relation Network to study the disaster image retrieval and detect the flood in satellite images. Zha et al. [69] used a CNN model trained on images to analyze flood videos captured from surface structures, key infrastructure, smart grids, homes, and buildings. The authors sorted the video with systematic exploration and used the CNN model to capture the video's Spatio-temporal features. The 3D-CNN technique is used in various studies that use 3D kernels, which stack the adjacent frames of an input video and convolve [70]. Simonyan [71] controlled the video's spatial and temporal components using a two-stream approach in which two different CNN models with different inputs were utilized. One input consisted of a Red-Green-Blue (RGB) frame for capturing spatial features, while the other was composed of multiple frames and dense optical flow to capture temporal features in the video. Calculating the weight of both streams provides the final output of the image. Ye et al. [72] used the same two streams neural network approach and applied evaluation methods such as parameters or fusion and prediction methods.

Various methods of image segmentation have been presented during the past few decades. These methods utilize context and neighborhood information for image classification. For this purpose, first, the pixels are combined into larger and meaningful image objects as a single-pixel cannot provide precise semantic information [73]. The pixels are then expanded into objects by considering the properties of texture, size, and distance of the image [74]. Fully Convolutional Network (FCN) models have been used on traditional aerial imagery by semantic segmentation [75,76]. Fu et al. [77] used the FCN model to classify high-resolution satellite images and calculated the precision, recall, and kappa coefficient as 0.81, 0.78, and 0.83, respectively, which were found to be significant. Nguyen et al. [78] utilized a five-layered network algorithm to classify satellite images and obtained an average classification accuracy of 83%. Another experiment achieved 91% accuracy where the Cafenet and GoogleNet CNN architectures were utilized. These were integrated with three different learning modalities required to classify land use images obtained by RS [79].

Furthermore, deep learning applications have also been reported where hyperspectral images are used, and their classification results have proven to be better than the SVM [80]. For example, the use of SVM and deep neural networks for flood prediction has been explored by Sankaranarayanan et al. [41]. The monsoon parameters, such as rainfall intensity and temperature, are used for training. According to the results, the deep neural network achieved an accuracy of 91.18%, while the SVM yielded 85.57% accuracy. Similarly, in another study, deep learning models such as CNN yielded better performance than SVM and random forests for the land use classification using RGB images [81].

From the literature, the use of deep learning models for image retrieval, classification, and segmentation is evident, and results have shown superior performance to the traditional image processing and machine learning models. Thus, the current study focuses on using deep learning, specifically CNN, to detect floods from aerial imagery captured through UAVs. The aim is to bring performance improvement and explore the application of deep learning for flood detection to devise proper and swift disaster response plans. The state-of-the-art UAVs have a built-in FPGS and parallel processors as hardware, which carry out feature extraction after capturing an image. Since CNN is less extensive due to the PL, it has been used in the current study to simplify image segmentation, feature classification, or texture classification. Furthermore, the CNN method is quite robust and fast, making it the preferred method in the current study.

3. Materials and Methods

A detailed study of the literature was conducted to understand the current technologies used for flood detection. The purpose was to identify the current technologies, their

utilization, and find existing gaps in the literature. The literature was retrieved from Google Scholar, Emerald Insight, Springer, Taylor and Francis library, ASCE, ACM, MDPI, Web of Science, and Scopus repositories. The search period was restored to literature published post-2010 to keep a recent focus on literature. The search strings utilized included "flood detection using machine learning" and "flood using deep learning", "SVM for flood detection" coupled with the terms CNN, RNN, and LSTM. A limit of English language and articles published as research papers only was applied to yield 148 articles. Similar methods have been used in recent studies for retrieving relevant literature [5,7,82].

According to the extensive literature review in the current study, Machine learning has emerged as a promising domain for disaster prediction and management. Deep learning is a subset of machine learning that uses a multilayer network of neurons to automatically extract features from an image, learn about the features, and classify them. In the current study, CNN and some other techniques have been used to detect floods from multispectral aerial images captured from the Indus River located in Pakistan. Figure 1 shows the overall methodology followed for flood detection from aerial images. Aerial images to be used as input to the CNN model are collected through UAVs from the target region. Images can also be retrieved and used from online sources such as Google Earth or social media. These images belong to two classes: Pre- and Post-disaster. The spatial information of both sets of images is identical. However, they have a difference in their time series. For example, one image may be captured in 2011, whereas the other is taken in 2016.
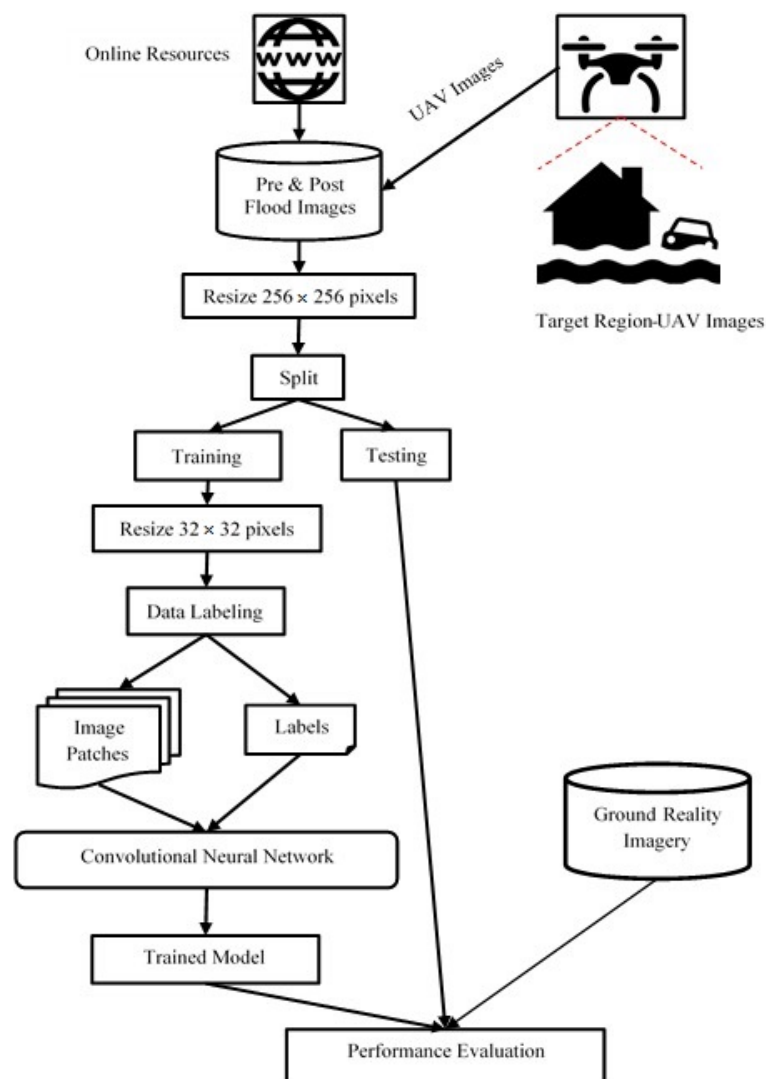

Figure 1. Proposed Methodology.

After acquiring images of the target location, the system underwent two phases: training and testing. The alterations of pre-disaster and post-disaster images are used as the input training patches. The goal is to observe and identify flood-related changes in the post-disaster images. The model learned these differences between pre-and post-disaster images as the image features for detecting the change. In previous studies, such as those presented by Joshi et al. [31], only pre-disaster imagery was used for flood detection.

In contrast, other studies either utilized pre- or post-disaster images, making it difficult to perform change detection, which led to errors at the initial stage. Therefore, in this research, the learning phase is improved and made error-free by incorporating both pre- and post-disaster imagery. The disaster-related changes identified in the output reveal the occurrence of disasters. Both pre-and post-disaster images are three-channeled RGB images, making the training patch with six channels. This results in enhanced precision and higher accuracy in performance. A similar study utilized four-channel input images, i.e., RGB and InfraRed (IR), to support their inner layer [83].

Figure 2 represents the complete architecture of the current study model for fast and accurate detection of flooded regions. The CNN architecture proposed in this research is inspired by AlexNet architecture. It consists of three convolution layers, three pooling layers, and two fully connected layers. CL, PL, and Fully Connected layers (FC) are represented in the architecture diagram by C, P, and FC, respectively. CL is used to extract different features such as edges and texture from images. These features are learned from the pre- and post-flood images to recognize the differences between both types of images to be classified accurately. An activation function follows each CL. Here a RELU activation function has been used with convolutional layers. PL reduces the number of parameters in the case of large-sized images, thus reducing their dimensions. This makes the learning process less extensive. Finally, the output from the previous layers is flattened and fed to the FC, which contains an activation function, i.e., softmax, to generate the final classification output.
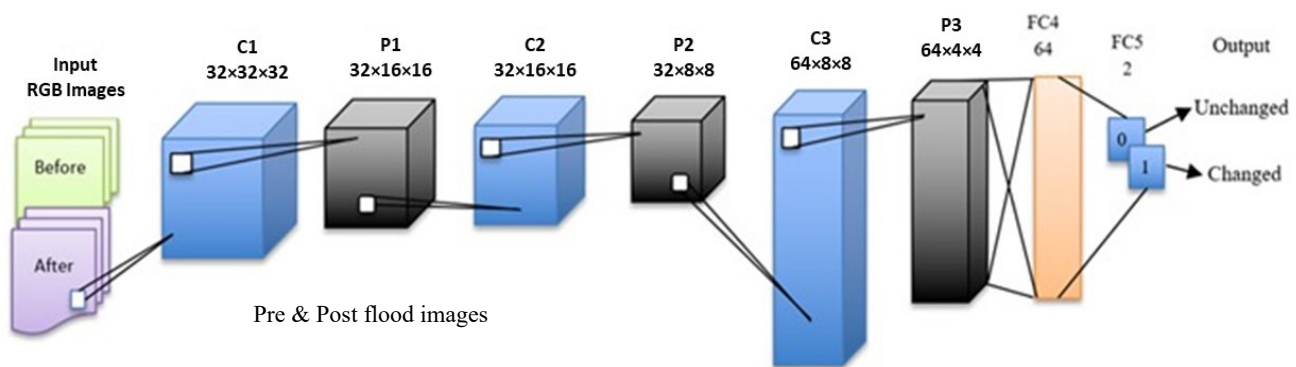

Figure 2. Base CNN Architecture.

3.1. Data Collection and Target Area

The target area for this study is the Indus River, located in Pakistan, which is among the longest rivers in Asia. It flows through China, India, and Pakistan. The current study's target area is the Indus Basin in Punjab, Pakistan, as shown in Figure 3. According to a United Nations report, the Indus River has been affected by severe flooding resulting in 1980 fatalities and impacted 18 million people in Pakistan. In addition, approximately 1.6 million families have been displaced during the floods due to either damage or destruction of their homes [84]. Furthermore, most of the population is directly affected due to the damages to homes, real estate, properties, and buildings. Therefore, the Indus Basin is one of the most flood-prone regions of Pakistan and is selected for the current study to examine the effects of flood disasters in this region and accurately map the flood-affected regions in case of any future disaster.

Figure 3. Indus River and the Case study area on the map of Pakistan.

Image data for the dataset is collected from UAV-based images and online sources such as Google Earth. It consists of both pre- and post-flood images. As images in the collected dataset had varying sizes and resolutions, each image was resized to 256 × 256 pixels to have uniform imagery for training. Two sets of images are created for the experiments, which are training and testing sets. The training set consists of 10 subsets, each containing 2150 patches. The testing set consists of 14 sets, having 2150 patches in each set. All images in the training dataset are of the same size and position. In addition, the alignment of images from both pre-and post-disaster categories and the ground truth imagery is the same. This is because the system requires inputs with constant dimensionality. For training, images can be of varying intensities. The query image for testing can also be of different intensity, alignment, and location so that the system performance can be tested for varying inputs.

3.2. Experimental Setup

Experiments are conducted on an HP Envy ×360 laptop with Intel core™ i7, 2.7 GHz base clock speed, and 8 GB RAM. The operating system is Windows 10, with an AMD Radeon R7 M265 graphics processor. The deep learning framework Convolutional Archi-

tecture for Fast Feature Embedding (Caffe) and the CNN architecture of AlexNet were utilized in the study.

On this platform, the Caffe framework is used as a deep learning model. It is a deep learning framework written in C++ and has an interface based on python. It is specifically developed for deep learning models focused on image classification and segmentation tasks. Therefore, it has a high processing speed and can do processing on a large number of images [85]. Figure 4 shows the implementation of CNN to build a deep learning model based on the Caffe framework. First, the flood data patches obtained from both pre- and post-flood images are used to train a CNN model. Second, the Caffe framework is used as a deep learning model after the CNN learning phase. Finally, the Caffe framework is used in the testing phase to classify disaster and non-disaster regions from a query image. Furthermore, a new image is provided to this model that is classified as either flooded or non-flooded.
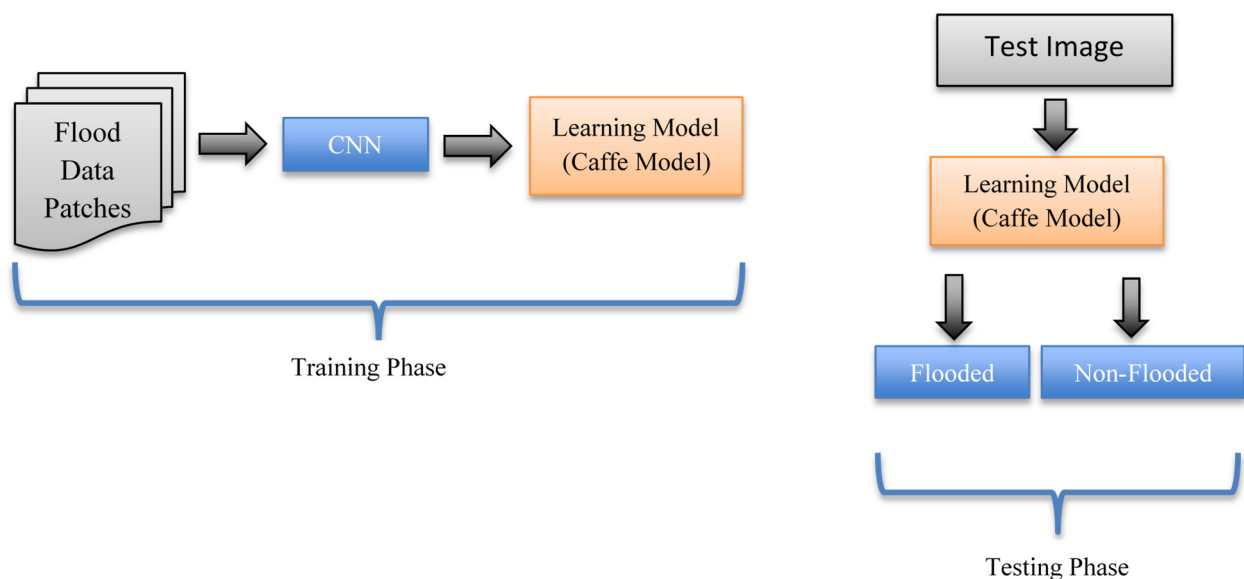

Figure 4. Overview of Training and Testing Process using Caffe Framework.

3.3. Training Phase

The learning of the system is carried out in the training phase (shown in Figure 5). Accordingly, all the possible features and characteristics of a certain geographical change or damage to homes and buildings or critical infrastructure caused by floods are studied in detail. At this point, the CNN approach is used for the detection of disasters. The first step of this phase is creating training patches made by trimming the pre-and post-disaster images and the images of ground reality from a particular disaster scene. The images obtained from the flooded land area of 256×256 pixels are cropped to 32×32 pixels patches in the current study. By trimming the images, 2150 patches are obtained from a single aerial image captured through UAV on the surface or homes and buildings. Next, the training patches are aligned in a top to the bottom position, as represented in Figure 5. The process is repeated for both pre-and post-disaster image patches. After alignment, a comparison is made between the combined disaster training patches and the patches of ground reality. The training patches are subsequently labeled as 0 or 1. Number "zero" is allotted when the change rate, i.e., the white region in the ground reality patches, is less than or equal to 15%, whereas "one" is allotted on the change rate greater than 10%. Thus, 0 represents the occurrence of significant change in the image, whereas 1 represents no change. In other words, 0 highlights the occurrence of a disaster, whereas 1 represents no disaster. After labeling the training patches, the images are saved and used to train the CNN model. CNN is trained for the data of more than 250,000 iterations, and the log is maintained.
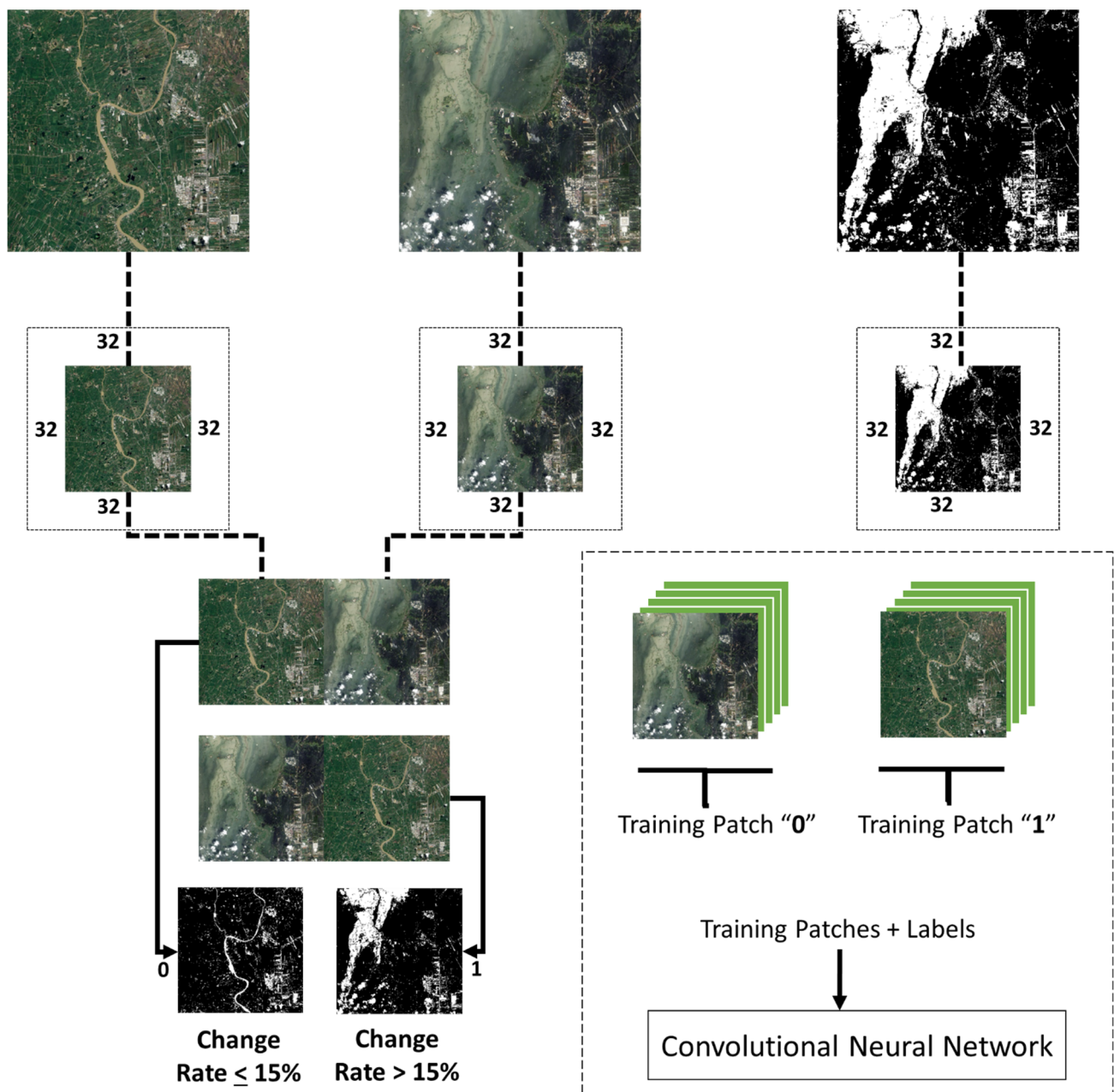
Figure 5. The training phase of the proposed method.

3.4. Testing Phase

The test phase is necessary to detect and evaluate the disaster-affected regions to plan an effective disaster response. As shown in Figure 6, the disaster detection results are extracted and prepared for the national disaster agency to work on. For successful operation and faster output delivery to the operator, the testing phase first merges the RGB channels of pre- and post-disaster images from the testing phase into a single image. The prediction value for disaster incidence is calculated using a raster scan over the image by sliding it over 16 pixels. From the previous predictions of the training phase, the patches with the "1" label are extracted and assembled to make a 32×32 pixel sized rectangle representing the actual disaster region. The method results are compared with actual on-ground images that underwent a raster scan on a 32×32 pixels region of interest for enhanced accuracy. Afterward, the performance is evaluated by three parameters: precision, recall, and f-score. Precision calculates how many positive predictions belong to the positive class. The recall

represents the number of positive predictions out of all the positive samples. F1-score provides a numeric value to balance the precision and recall concerns. The performance assessment measures are calculated as shown in Equations (1)–(3):

$$Recall = \frac{TruePositive}{TruePositive + FalseNegative} \tag{1}$$

$$Precision = \frac{TruePositive}{TruePositive + FalsePositive} \tag{2}$$

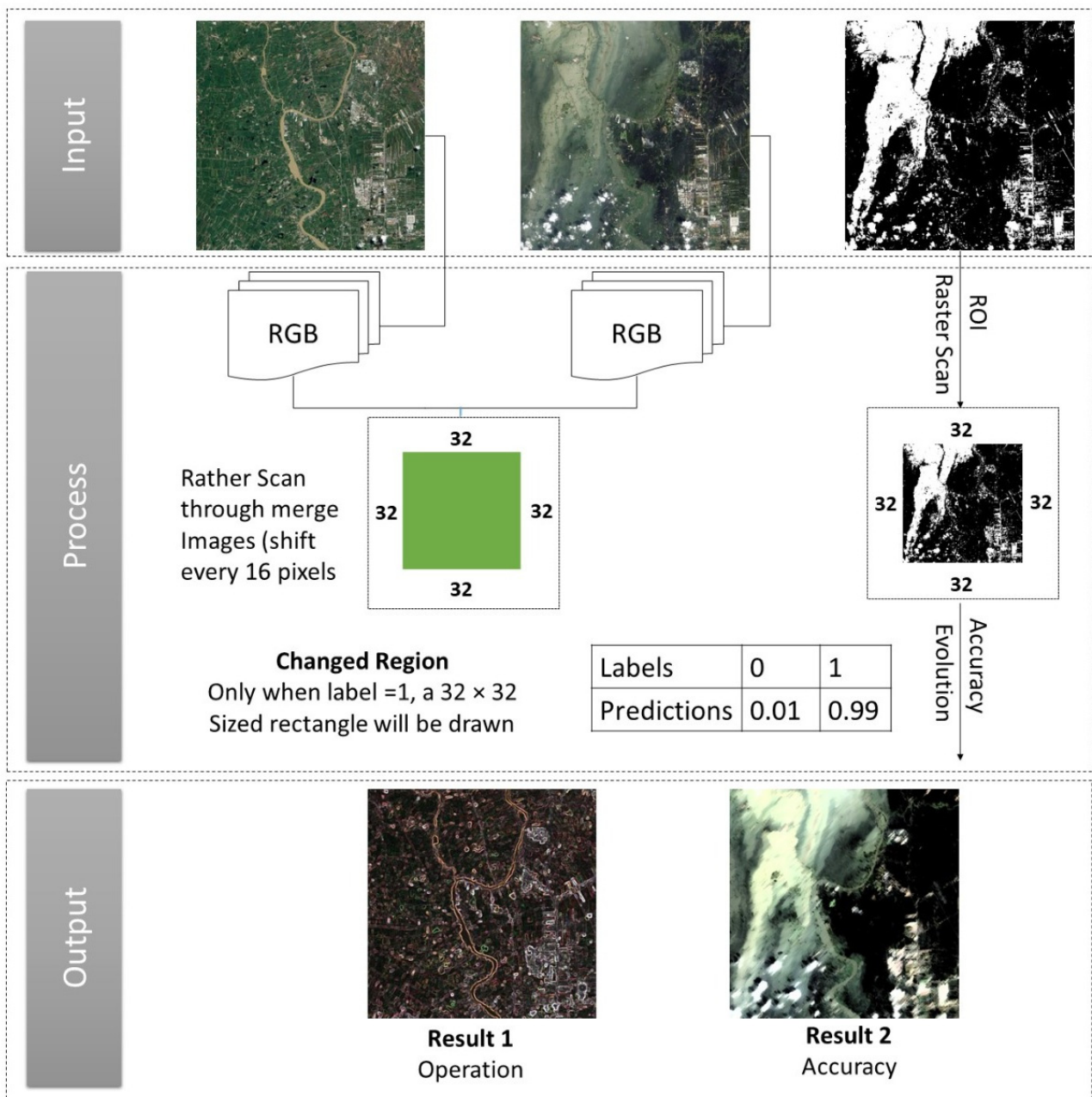$$F1 - Score = 2 \times \frac{Precision \times Recall}{Precision + Recall} \tag{3}$$

Figure 6. The testing phase of the proposed method.

Again, the test log is maintained for reference.

The data acquisition by UAVs through digital aerial photography has certain features. The day and night surveillance over the target area is carried out using infrared thermal imaging. A drone requires two-axis gyro stability, with the calculation of target location and tracking target image. The real-time monitoring of the location can be carried out during day or night by combing thermal imaging and visible light. The target can be captured and located automatically with the help of the image feature or lock table. Overall, the UAV used in such studies should have the characteristics as shown in Table 2.

Table 2. UAV characteristics.

Components	Specifications
Hardware	2-axes Stabilization, EO/IR Lightweight contraction mechanism with shock absorbers, Azimuth angle of N $\times$ 360°, tilt between $-130°\sim+90°$ and maximum angular rate of $\geq 60°/\text{s}$
EO	Pixel of 1920 $\times$ 1080, optical zoom up to 30 times and digital zoom up to 12 times
IR	Pixel of 640 $\times$ 480, Vanadium oxide sensor, 8 um–12 um spectrum, and 25 mm lens
Recording	H.264 Coding TS. Packages

4. Results and Discussions

Five segments of aerial images captured through UAVs in the affected areas are involved for each input image in the dataset. These are pre- or post-disaster images, training inputs to the model, ground truth images, segmentation outputs, and the final flood detection results illustrating the various performance metrics, as shown in Figures 7 and 8. Calculation of accuracy is important, and its high value determines the reliability of the system. It is calculated by various parameters such as true-positive (represented in red color in Figures 7 and 8, true-negative (blue color), false-positive (green color), and false negative (yellow color). These parameters are required to calculate precision, f-score, and recall, which are performance metrics for disaster detection.

Flood is detected from the test images with high accuracy and robustness. The two sets of flood detection results represented in Figures 7 and 8 show images captured at the Indus River Region in Pakistan.

Figure 7 shows results on an input test image captured from the Indus River basin region I. As shown in this Figure 7, nearly all the flooded regions are successfully detected by the system. Figure 8 shows the results obtained from an image captured from the Indus River region II. Some small regions in the rooftops are falsely highlighted as flooded, while some regions containing shadows are falsely perceived as land by the system, as shown in the output image (d). Such errors can be avoided by using appropriate pre-processing steps on images such as shadow and noise removal. However, apart from some minor false detections, the system has correctly recognized all major flooded regions.
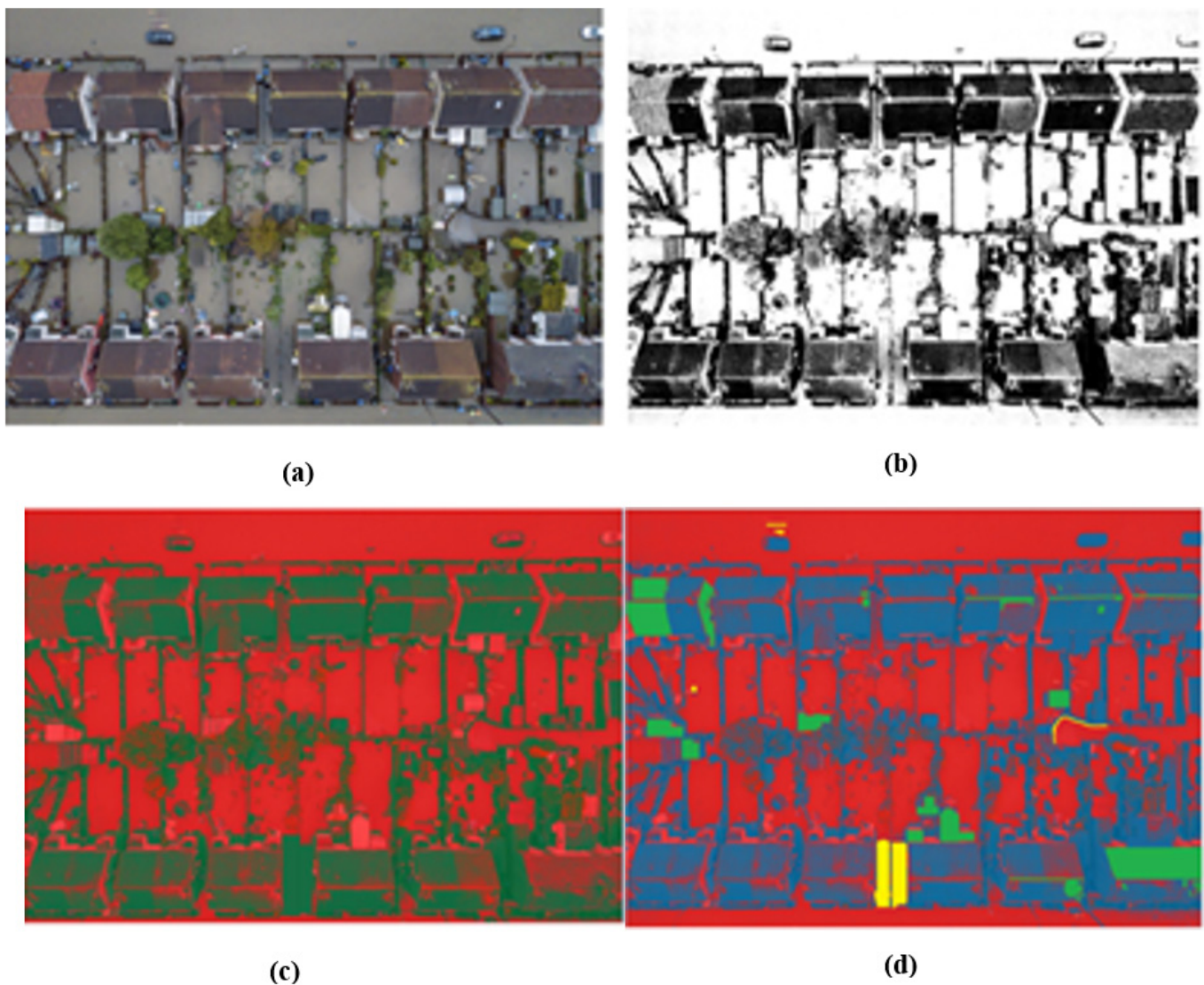
Figure 7. Flood Detection Results at Indus River Region I. (**a**) Input Image (**b**) Ground Reality (**c**) Segmentation Results (**d**) Output Image, True-Positive (Red), True-Negative (Blue), False-Positive (Green), False-Negative (Yellow).

Training and Testing Rates

The system demonstrates an adept training rate, with a loss rate of 0.4 at 250,000 iterations, manifested by the AlexNet model—the loss function defects how well specific algorithm models the given data. If predictions deviate too much from actual results, a loss would be higher and vice versa. Equation (4) presents the losses in the current study.

$$Loss = \frac{\sum_{i=1}^{n}(yi - zi)^2}{n} \tag{4}$$

where n is the number of training examples, i is the ith training example in a data set, yi is the ground truth label for ith training example, and zi prediction for ith training.
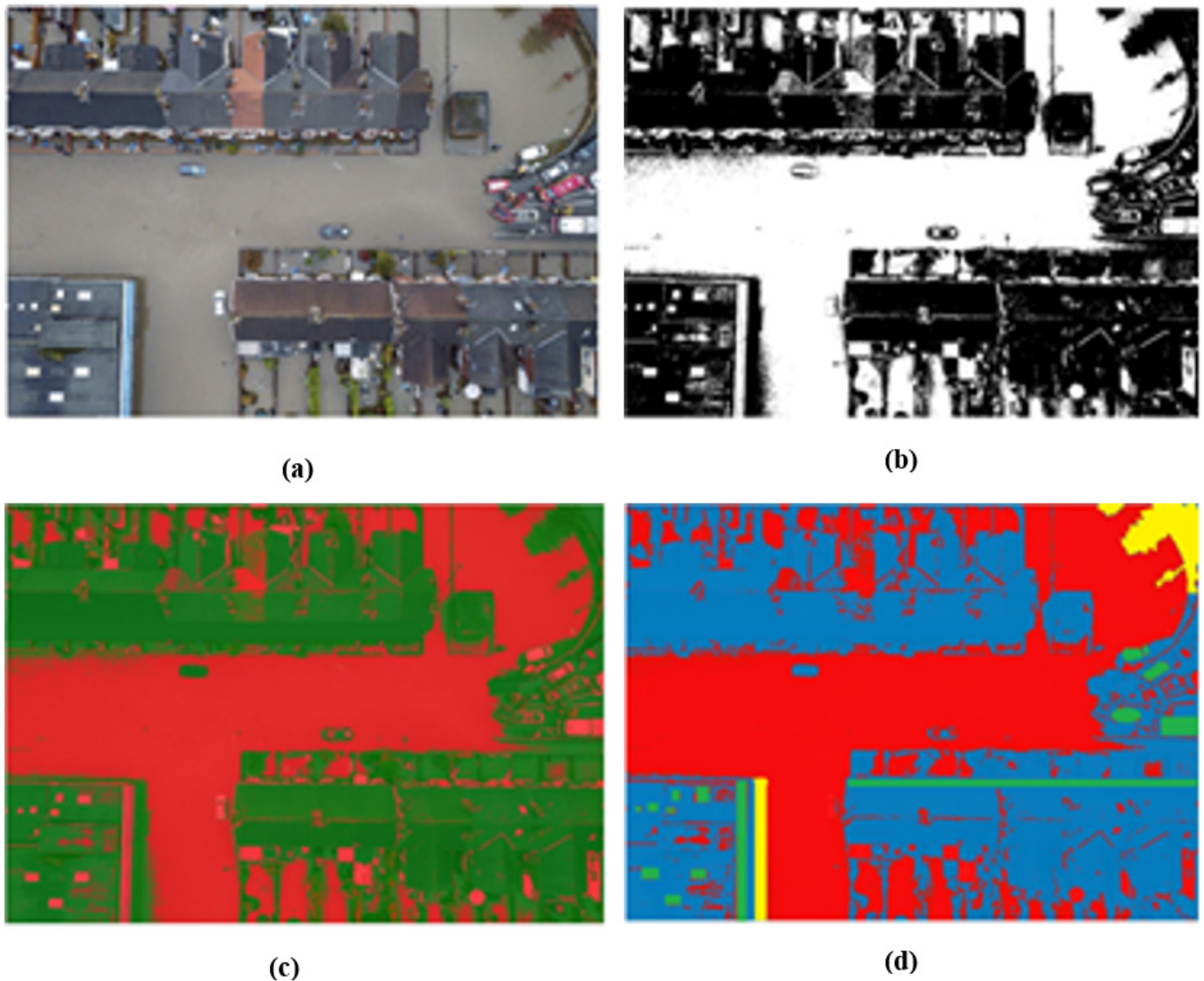
Figure 8. Flood Detection Results at Indus River Region II. (**a**) Input Image (**b**) Ground Reality (**c**) Segmentation Results (**d**) Output Image, True Positive (Red), True Negative (Blue), False Positive (Green), False Negative (Yellow).

A stable training rate is achieved after 10,000 iterations, as depicted in Figure 9. A computing time of 9 min is required for learning at 250,000 iterations as the GPU accelerates the learning time. For a stable testing rate, 10,000 iterations are made with an accuracy of 0.82, as shown in Figure 10. Conversely, 250,000 iterations had an accuracy rate of 0.91. It took 6 s to test an image of 256 × 256 pixels.

Table 3 summarizes the flood detection results. The proposed model achieved an overall accuracy of 91% in all the patches of the dataset available. Lopez-Fuentes [68] developed a system to detect floods from social media posts using a deep learning-based CNN model to retrieve visual features and a bi-directional LSTM model. The system achieved an accuracy of 84%. In comparison, the current study achieved a higher accuracy rate; thus, a single CNN model can yield higher accuracy than the approach that incorporated both CNN and LSTM.
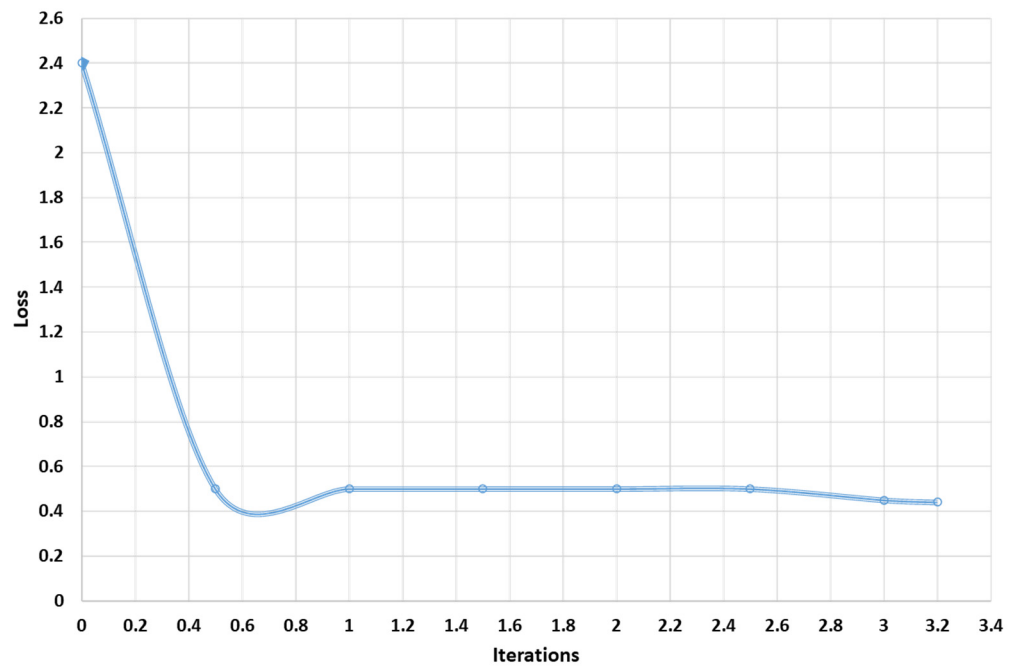
Figure 9. Training rate of the model. Note: the *x*-axis represents the number of iterations, and *Y*-axis represents a loss.
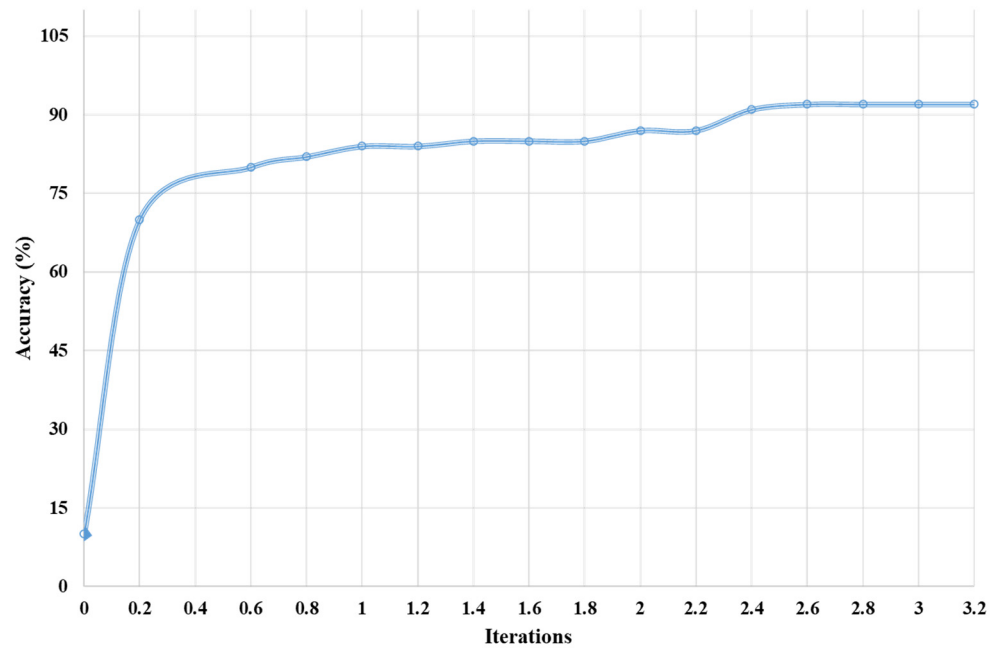

Figure 10. Testing rate of the model. Note: the *x*-axis represents the number of iterations, and *Y*-axis represents the accuracy.

Table 3. Flood Detection Results.

Region	Precision (P)	Recall (R)	F1-Score (F)
Indus River I (Figure 7)	0.84	0.91	0.87
Indus River II (Figure 8)	0.93	0.75	0.83

At the end of the research, a test is conducted in a non-disaster region to check the system's authenticity. The test on a non-disaster region illustrates the system's capability to successfully distinguish between disaster and non-disaster regions, as no changes are seen in the output image with no color difference. Thus, the system gave accurate results and detected no disaster, as presented in Figure 11. This proves the authenticity of the system to distinguish between flooded regions and the river. Although the river and flood share the same color, the system was precise enough to detect differences between the two entities.

(a)　　　　　　　　　　　　　　　　　　　　　　　　　**(b)**

Figure 11. Test on a non-disaster region (**a**) Input Image (**b**) Output.

The flood has been detected from multispectral aerial images captured through UAV using a CNN model and automatic difference extraction in this research. It applies to all types of images, whether related to buildings or other infrastructure if the quality is consistent. For different sets of images, f1-scores of 0.83 and 0.87 are achieved. The method is successful in detecting disaster regions with high accuracy for both surface structures and agricultural lands. It depicts notable improvements in f-score, precision, and recall parameters. A similar study showed a 90% accuracy value using the CNN method to determine the flood incidence with classification [86]. Li et al. [46] used an active, self-learning CNN to detect flooded areas from SAR imagery. This model was used to overcome the impact of insufficient annotated data for training and recorded an accuracy of 86.91%.

In comparison, the method proposed in the current study shows better outcomes than other studies utilizing CNN for disaster management. Apart from accuracy, during image processing in the current study, all the six RGB channels are combined to obtain the disaster regions using the CNN model. Thus, no color information is lost during this process. Previously, work was done based on two channels: one pre- disaster channel having either R, G, or B channel or the same for the post-disaster image, which used a simple subtraction method. However, the current method with improved six channels retained the original color content of both pre-and post-disaster phases.

The accuracy of flood detection in the current study is further improved by eliminating ambiguity and misalignment in the results. For this purpose, the input dataset composing pre- and post-disaster imagery and the ground reality is first subjected to an aligned adjustment process. Then, the resulting data are passed on to the training phase. The data used in the presented model have the same color variation, and all images are taken on a sunny day. Having different color variations could create complexity. For example, if taken in cloudy weather, darker regions, or rainfall, the images can have color variations, making the detection process difficult. Therefore, before moving the images to the training phase, it is important to pre-process them and increase the variation to perform well in all sorts of weather conditions. Blaschke [29] utilized three different training strategies to train the CNN model for flood detection. Accordingly, in the current study, the RGB

channels and IR are normalized before the model's training to remove location bias due to environmental changes distorting the image.

For flood detection and damage assessment, both the image pattern and several training patches are considered as these factors strongly affect the final output's accuracy. Both these properties are directly proportional to the overall accuracy. For example, a study led by Ahmad et al. used many training samples whose quantity was increased by performing augmentation operations on the images. The operations include horizontal and vertical flipping and changing brightness levels at an interval of $\pm40\%$ [87]. Thus, many patterns and enormous training patches will ultimately result in higher accuracy and improved results adopted in the current study.

5. Conclusions

The current study uses a deep learning approach for detecting flooded areas in city infrastructure through UAV-captured images that have demonstrated excellent performance with an accuracy of 91%. The results have been compared with existing methods to illustrate a significant improvement over the previous flood detection model. The method proposed in this paper is useful in detecting and extracting the flooded regions in input images. It can be implemented in every disaster management situation and adopted by the global disaster response and relief organizations. The model can help detect the disaster area in an emergency and narrow down the search process so that relief routes can be determined immediately, and support can be provided to the people affected in the disaster region. Hence, casualties can be reduced, and rescue operations can be initiated immediately by the responsible organization. It is equally applicable to structures and agricultural land where the images can be captured through UAVs from the flooded region. This project can also serve as a cost-effective solution for flood detection and, therefore, assist developing countries in post-flood relief activities by quickly identifying and locating inundated areas. Other countries frequently affected by flood disasters can also benefit from this system.

One limitation of the system is that some minor false detections are noticed when shadows and other noisy pixels are classified as flooded regions. This is particularly evident in darker spaces that may appear like water and misclassified as a flooded regions. However, using sophisticated cameras in UAVs with inbuilt flashes and high-performance image enhancement and editing tools. In further work on the proposed system, noise and shadow removal techniques can be imposed in the pre-processing phase to improve the performance. In the future, the dataset can be improved and enhanced through the addition of more training images. The accuracy of the system can be noticeably enhanced by expanding the training dataset. This can be done by capturing more images, varying in scale, color, illumination, and other physical properties so that the system can work precisely under a diverse collection of test images. This will add to the versatility of the system as well as improve its performance.

Author Contributions: Conceptualization, H.S.M. and F.U.; methodology, H.S.M., F.U., S.Q.; software, H.S.M., F.U.; validation, H.S.M., F.U., S.Q., S.I.K. and M.M.; formal analysis, H.S.M. and F.U.; investigation, H.S.M. and F.U.; resources, H.S.M., F.U. and M.M.; data curation, H.S.M., F.U., S.Q., S.I.K. and M.M.; writing—original draft preparation, H.S.M. and F.U.; writing—review and editing, H.S.M., F.U., S.Q., S.I.K. and M.M.; visualization, H.S.M. and F.U.; supervision, F.U. and M.M.; project administration, H.S.M. and F.U.; funding acquisition, M.M. All authors have read and agreed to the published version of the manuscript.

Institutional Review Board Statement: Not applicable.

Informed Consent Statement: Not applicable.

Data Availability Statement: The data is available with the first author and can be shared with anyone based on a reasonable request.

Conflicts of Interest: The authors declare no conflict of interest.

References

1. Veh, G.; Korup, O.; Walz, A. Hazard from Himalayan glacier lake outburst floods. *Proc. Natl. Acad. Sci. USA* **2020**, *117*, 907–912. [CrossRef] [PubMed]
2. Lim, H.R.; Lim, M.B.B.; Piantanakulchai, M. Determinants of household flood evacuation mode choice in a developing country. *Nat. Hazards* **2016**, *84*, 507–532. [CrossRef]
3. Ritchie, H.; Roser, M. Natural Disasters. Available online: https://ourworldindata.org/natural-disasters (accessed on 19 October 2020).
4. Munawar, H.S.; Hammad, A.; Ullah, F.; Ali, T.H. After the flood: A novel application of image processing and machine learning for post-flood disaster management. In Proceedings of the 2nd International Conference on Sustainable Development in Civil Engineering (ICSDC 2019), Jamshoro, Pakistan, 5–7 December 2019.
5. Munawar, H.S.; Qayyum, S.; Ullah, F.; Sepasgozar, S. Big Data and Its Applications in Smart Real Estate and the Disaster Management Life Cycle: A Systematic Analysis. *Big Data Cogn. Comput.* **2020**, *4*, 4. [CrossRef]
6. Fajardo, J.T.B.; Yasumoto, K.; Ito, M. Content-based data prioritization for fast disaster images collection in delay tolerant network. In Proceedings of the 2014 Seventh International Conference on Mobile Computing and Ubiquitous Networking (ICMU), Institute of Electrical and Electronics Engineers (IEEE). Singapore, 6–8 January 2014; pp. 147–152.
7. Azeem, M.; Ullah, F.; Thaheem, M.J.; Qayyum, S. Competitiveness in the construction industry: A contractor's perspective on barriers to improving the construction industry performance. *J. Constr. Eng. Manag. Innov.* **2020**, *3*, 193–219. [CrossRef]
8. Ullah, F.; Sepasgozar, S.M.E. A Study of Information Technology Adoption for Real-Estate Management: A System Dynamic Model. *Innov. Prod. Constr.* **2019**, 469–486. [CrossRef]
9. Ullah, F.; Sepasgozar, S.M.E.; Wang, C. A Systematic Review of Smart Real Estate Technology: Drivers of, and Barriers to, the Use of Digital Disruptive Technologies and Online Platforms. *Sustainability* **2018**, *10*, 3142. [CrossRef]
10. Munawar, H.S. Image and Video Processing for Defect Detection in Key Infrastructure. *Mach. Vis. Insp. Syst.* **2020**, *1*, 159–177. [CrossRef]
11. Smith, A. 2017 U.S. Billion-Dollar Weather and Climate Disasters: A Historic Year in Context. Available online: https://www.climate.gov/news-features/blogs/beyond-data/2017-us-billion-dollar-weather-and-climate-disasters-historic-year (accessed on 19 October 2020).
12. Shrestha, B.B.; Sawano, H.; Ohara, M.; Yamazaki, Y.; Tokunaga, Y. Methodology for Agricultural Flood Damage Assessment. In *Recent Advances in Flood Risk Management*; IntechOpen: London, UK, 2019.
13. FAO. Damage and Losses from Climate-Related Disasters in Agricultural Sectors. Available online: http://www.fao.org/3/a-i6486e.pdf (accessed on 25 January 2021).
14. FEMA. Flood Safety Awareness and American Red Cross Month. In *Stakeholder Toolkit*; US Department of Commerce, National Oceanic and Atmospheric Administration; National Weather Service: Washington, DC, USA, 2018.
15. Felli, F.; Liu, C.; Ullah, F.; Sepasgozar, S. Implementation of 360 videos and mobile laser measurement technologies for immersive visualisation of real estate & properties. In Proceedings of the 42nd AUBEA Conference, Singapore, 26–28 September 2018.
16. Low, S.; Ullah, F.; Shirowzhan, S.; Sepasgozar, S.M.; Lee, C.L. Smart Digital Marketing Capabilities for Sustainable Property Development: A Case of Malaysia. *Sustainability* **2020**, *12*, 5402. [CrossRef]
17. Ullah, F.; Sepasgozar, P.S.; Ali, T.H. Real estate stakeholders technology acceptance model (RESTAM): User-focused big9 disruptive technologies for smart real estate management. In Proceedings of the 2nd International Conference on Sustainable Development in Civil Engineering (ICSDC 2019), Jamshoro, Pakistan, 5–7 December 2019.
18. Munawar, H.S.; Maqsood, A. Isotropic surround suppression based linear target detection using hough transform. In Proceedings of the International Conference on Cultural Technologies (ICCT 2017), Chiang Mai, Thailand, 12–14 January 2017; pp. 357–361.
19. Qayyum, S.; Ullah, F.; Al-Turjman, F.; Mojtahedi, M. Managing smart cities through six sigma DMADICV method: A review-based conceptual framework. *Sustain. Cities Soc.* **2021**, *72*, 103022. [CrossRef]
20. Ullah, F.; Sepasgozar, S.M.; Shirowzhan, S.; Davis, S. Modelling users' perception of the online real estate platforms in a digitally disruptive environment: An integrated KANO-SISQual approach. *Telemat. Inform.* **2021**, *63*, 101660. [CrossRef]
21. Ullah, F.; Sepasgozar, S.M.; Thaheem, M.J.; Wang, C.C.; Imran, M. It's all about perceptions: A DEMATEL approach to exploring user perceptions of real estate online platforms. *Ain Shams Eng. J.* **2021**. [CrossRef]
22. Pan, J.; Yin, Y.; Xiong, J.; Luo, W.; Gui, G.; Sari, H. Deep Learning-Based Unmanned Surveillance Systems for Observing Water Levels. *IEEE Access* **2018**, *6*, 73561–73571. [CrossRef]
23. Atif, S.; Umar, M.; Ullah, F. Investigating the flood damages in Lower Indus Basin since 2000: Spatiotemporal analyses of the major flood events. *Nat. Hazards* **2021**, 1–27. [CrossRef]
24. Munawar, H.S.; Zhang, J.; Li, H.; Mo, D.; Chang, L. Mining Multispectral Aerial Images for Automatic Detection of Strategic Bridge Locations for Disaster Relief Missions. In *Trends and Applications in Knowledge Discovery and Data Mining*; Springer: Berlin, Germany, 2019.
25. Munawar, S.H.; Maqsood, A.; Mustansar, Z. Isotropic surround suppression and Hough transform based target recognition from aerial images. *Int. J. Adv. Appl. Sci.* **2017**, *4*, 37–42. [CrossRef]

26. Qadir, Z.; Ullah, F.; Munawar, H.S.; Al-Turjman, F. Addressing disasters in smart cities through UAVs path planning and 5G communications: A systematic review. *Comput. Commun.* **2021**, *168*, 114–135. [CrossRef]
27. Gebrehiwot, A.; Hashemi-Beni, L.; Thompson, G.; Kordjamshidi, P.; Langan, T.E. Deep Convolutional Neural Network for Flood Extent Mapping Using Unmanned Aerial Vehicles Data. *Sensors* **2019**, *19*, 1486. [CrossRef]
28. Munawar, H.S. Flood Disaster Management: Risks, Technologies, and Future Directions. In *Machine Vision Inspection Systems: Image Processing, Concepts, Methodologies and Applications*; Wiley: Hoboken, NJ, USA, 2020; Volume 1, pp. 115–146.
29. Blaschke, T. What's Wrong with Pixels? *Some Recent Developments Interfacing Remote Sens. Gis.* **2001**, *6*, 12–17.
30. Pradhan, B.; Tehrany, M.S.; Jebur, M.N. A New Semiautomated Detection Mapping of Flood Extent from TerraSAR-X Satellite Image Using Rule-Based Classification and Taguchi Optimization Techniques. *IEEE Trans. Geosci. Remote Sens.* **2016**, *54*, 4331–4342. [CrossRef]
31. Joshi, A.R.; Tarte, I.; Suresh, S.; Koolagudi, S.G. Damage identification and assessment using image processing on post-disaster satellite imagery. In Proceedings of the 2017 IEEE Global Humanitarian Technology Conference (GHTC), Institute of Electrical and Electronics Engineers (IEEE). Seattle, WA, USA, 17–20 October 2017; pp. 1–7.
32. Rizeei, H.M.; Pradhan, B.; Saharkhiz, M.A. An integrated fluvial and flash pluvial model using 2D high-resolution sub-grid and particle swarm optimization-based random forest approaches in GIS. *Complex Intell. Syst.* **2019**, *5*, 283–302. [CrossRef]
33. Lyu, H.-M.; Shen, S.-L.; Zhou, A.; Yang, J. Perspectives for flood risk assessment and management for mega-city metro system. *Tunn. Undergr. Space Technol.* **2019**, *84*, 31–44. [CrossRef]
34. Ireland, G.; Volpi, M.; Petropoulos, G.P. Examining the Capability of Supervised Machine Learning Classifiers in Extracting Flooded Areas from Landsat TM Imagery: A Case Study from a Mediterranean Flood. *Remote Sens.* **2015**, *7*, 3372–3399. [CrossRef]
35. Sutskever, I.; Hinton, G.E. Deep, Narrow Sigmoid Belief Networks Are Universal Approximators. *Neural Comput.* **2008**, *20*, 2629–2636. [CrossRef] [PubMed]
36. Krizhevsky, A.; Sutskever, I.; Hinton, G. Magenet classification with deep convolutional neural networks. In Proceedings of the Advances in Neural Information Processing Systems, Lake Tahoe, NV, USA, 3–6 December 2012; pp. 1097–1105.
37. Anuse, A.; Vyas, V. A novel training algorithm for convolutional neural network. *Complex Intell. Syst.* **2016**, *2*, 221–234. [CrossRef]
38. Grossberg, S. Recurrent neural networks. *Scholarpedia* **2013**, *8*, 1888. [CrossRef]
39. Kollias, D.; Tagaris, A.; Stafylopatis, A.; Kollias, S.; Tagaris, G. Deep neural architectures for prediction in healthcare. *Complex Intell. Syst.* **2018**, *4*, 119–131. [CrossRef]
40. Jabbari, A.; Bae, D.-H. Application of Artificial Neural Networks for Accuracy Enhancements of Real-Time Flood Forecasting in the Imjin Basin. *Water* **2018**, *10*, 1626. [CrossRef]
41. Sankaranarayanan, S.; Prabhakar, M.; Satish, S.; Jain, P.; Ramprasad, A.; Krishnan, A. Flood prediction based on weather parameters using deep learning. *J. Water Clim. Chang.* **2020**, *11*, 1766–1783. [CrossRef]
42. Doubleday, J.; McLaren, D.; Chien, S.; Lou, Y. Using Support Vector Machine Learning to Automatically Interpret Modis, Ali, And L-Band Sar Remotely Sensed Imagery For Hydrology, Land Cover, And Cryosphere Applications. In Proceedings of the Workshop on AI and Space, International Joint Conference on Artificial Intelligence, Barcelona, Spain, 16–22 July 2011.
43. Elsafi, S.H. Artificial Neural Networks (ANNs) for flood forecasting at Dongola Station in the River Nile, Sudan. *Alex. Eng. J.* **2014**, *53*, 655–662. [CrossRef]
44. Anusha, N.; Bharathi, B. Flood detection and flood mapping using multi-temporal synthetic aperture radar and optical data. *Egypt. J. Remote Sens. Space Sci.* **2020**, *23*, 207–219. [CrossRef]
45. Hosseiny, H.; Nazari, F.; Smith, V.; Nataraj, C. A Framework for Modeling Flood Depth Using a Hybrid of Hydraulics and Machine Learning. *Sci. Rep.* **2020**, *10*, 1–14. [CrossRef]
46. Li, Y.; Martinis, S.; Wieland, M. Urban flood mapping with an active self-learning convolutional neural network based on TerraSAR-X intensity and interferometric coherence. *ISPRS J. Photogramm. Remote Sens.* **2019**, *152*, 178–191. [CrossRef]
47. Zhao, G.; Pang, B.; Xu, Z.; Peng, D.; Zuo, D. Urban flood susceptibility assessment based on convolutional neural networks. *J. Hydrol.* **2020**, *590*, 125235. [CrossRef]
48. Basha, E.; Rus, D. Design of early warning flood detection systems for developing countries. In Proceedings of the 2007 International Conference on Information and Communication Technologies and Development, Institute of Electrical and Electronics Engineers (IEEE). Bangalore, India, 15–16 December 2007; pp. 1–10.
49. Alfieri, L.; Velasco, D.; Thielen, J. Flash flood detection through a multi-stage probabilistic warning system for heavy pre-cipitation events. *Adv. Geosci.* **2011**, *29*, 69–75. [CrossRef]
50. Narayanan, R.; Lekshmy, V.M.; Rao, S.; Sasidhar, K. A novel approach to urban flood monitoring using computer vision. In Proceedings of the Fifth International Conference on Computing, Communications and Networking Technologies (ICCCNT), Hefei, China, 11–13 July 2014; Institute of Electrical and Electronics Engineers (IEEE): Piscataway, NJ, USA, 2014; pp. 1–7.
51. Mousa, M.; Zhang, X.; Claudel, C. Flash Flood Detection in Urban Cities Using Ultrasonic and Infrared Sensors. *IEEE Sens. J.* **2016**, *16*, 7204–7216. [CrossRef]
52. Wang, Y.; Chen, A.; Fu, G.; Djordjevic, S.; Zhang, C.; Savić, D.A. An integrated framework for high-resolution urban flood modelling considering multiple information sources and urban features. *Environ. Model. Softw.* **2018**, *107*, 85–95. [CrossRef]
53. Smith, L.; Liang, Q.; James, P.; Lin, W. Assessing the utility of social media as a data source for flood risk management using a real-time modelling framework: Assessing the utility of social media for flood risk management. *J. Flood Risk Manag.* **2017**, *10*, 370–380. [CrossRef]

54. Amit, S.N.K.B.; Aoki, Y. Disaster Detection from Aerial Imagery with Convolutional Neural Network. In Proceedings of the 2017 International Electronics Symposium on Knowledge Creation and Intelligent Computing (IES-KCIC), Surabaya, Indonesia, 26–27 September 2017; pp. 239–245. [CrossRef]

55. Zhao, Y.; Wang, T.; Zhang, S.; Wang, Y. Towards minimum code dissemination delay through UAV joint vehicles for smart city. *IET Commun.* **2020**, *14*, 2442–2452. [CrossRef]

56. Islam, A.; Shin, S.Y. A blockchain-based secure healthcare scheme with the assistance of unmanned aerial vehicle in In-ternet of Things. *Comput. Electr. Eng.* **2020**, *84*, 106627. [CrossRef]

57. Kumar, S.J.; Kumar, S.; Choksi, M.; Zaveri, M.A. Collaborative data acquisition and processing for post disaster manage-ment and surveillance related tasks using UAV-based IoT cloud. *Int. J. Ad Hoc Ubiquitous Comput.* **2020**, *34*, 216–232. [CrossRef]

58. Ejaz, W.; Ahmed, A.; Mushtaq, A.; Ibnkahla, M. Energy-efficient task scheduling and physiological assessment in disaster management using UAV-assisted networks. *Comput. Commun.* **2020**, *155*, 150–157. [CrossRef]

59. Mehallegue, N.; Djellab, M.; Loukhaoukha, K. Efficient Use of UAVs for Public Safety in Disaster and Crisis Management. *Wirel. Pers. Commun.* **2020**, 1–12. [CrossRef]

60. Kastridis, A.; Kirkenidis, C.; Sapountzis, M. An integrated approach of flash flood analysis in ungauged Mediterranean watersheds using post-flood surveys and Unmanned Aerial Vehicles (UAVs). *Hydrol. Processes* **2020**. [CrossRef]

61. Liu, W.; Chen, Z.; Zheng, M. An Audio-Based Fault Diagnosis Method for Quadrotors Using Convolutional Neural Network and Transfer Learning. In Proceedings of the 2020 American Control Conference (ACC), Denver, CO, USA, 1–3 July 2020.

62. Rottondi, C.; Malandrino, F.; Bianco, A.; Chiasserini, C.F.; Stavrakakis, I. Scheduling of emergency tasks for multiservice UAVs in post-disaster scenarios. *Comput. Netw.* **2021**, *184*, 107644. [CrossRef]

63. Khosravi, K.; Panahi, M.; Golkarian, A.; Keesstra, S.D.; Saco, P.M.; Bui, D.T.; Lee, S. Convolutional neural network approach for spatial prediction of flood hazard at national scale of Iran. *J. Hydrol.* **2020**, *591*, 125552. [CrossRef]

64. Ali, H.; Choi, J.-H. A Review of Underground Pipeline Leakage and Sinkhole Monitoring Methods Based on Wireless Sensor Networking. *Sustainability* **2019**, *11*, 4007. [CrossRef]

65. Ahmed, H.; La, H.M.; Tran, K. Rebar detection and localization for bridge deck inspection and evaluation using deep residual networks. *Autom. Constr.* **2020**, *120*, 103393. [CrossRef]

66. Mason, D.C.; Speck, R.; Devereux, B.; Schumann, G.J.P.; Neal, J.C.; Bates, P.D. Flood Detection in Urban Areas Using Ter-raSAR-X. *IEEE Trans. Geosci. Remote Sens.* **2010**, *48*, 882–894. [CrossRef]

67. Di Martino, G.; Iodice, A.; Riccio, D.; Ruello, G. A Novel Approach for Disaster Monitoring: Fractal Models and Tools. *IEEE Trans. Geosci. Remote Sens.* **2007**, *45*, 1559–1570. [CrossRef]

68. Lopez-Fuentes, L.; Van de Weijer, J.; Bolanos, M.; Skinnemoen, H. Multi-modal deep learning approach for flood detection. In Proceedings of the MediaEval 2017 Workshop, Dublin, Ireland, 13–15 September 2017.

69. Zha, S.; Luisier, F.; Andrews, W.; Srivastava, N.; Salakhutdinov, R. Exploiting Image-trained CNN Architectures for Uncon-strained Video Classification. In Proceedings of the British Machine Vision Conference 2015, Swansea, UK, 7–10 September 2015; British Machine Vision Association: Swansea, UK, 2015; pp. 60.1–60.13.

70. Ji, S.; Xu, W.; Yang, M.; Yu, K. 3D Convolutional Neural Networks for Human Action Recognition. *IEEE Trans. Pattern Anal. Mach. Intell.* **2013**, *35*, 221–231. [CrossRef] [PubMed]

71. Simonyan, K.; Zisserman, A. Two-stream convolutional networks for action recognition in videos. In Proceedings of the NIPS'14: Proceedings of the 27th International Conference on Neural Information Processing Systems, Montreal, QC, Canada, 8–13 December 2014.

72. Ye, H.; Wu, Z.; Zhao, R.-W.; Wang, X.; Jiang, Y.-G.; Xue, X. Evaluating Two-Stream CNN for Video Classification. In Proceedings of the 5th ACM on International Conference on Multimedia Retrieval, Association for Computing Machinery (ACM). Shanghai, China, 23–26 June 2015; pp. 435–442.

73. Sande, V.C.; Jong, D.S.; Roo, D.A. A segmentation and classification approach of IKONOS-2 imagery for land cover mapping to assist flood risk and flood damage assessment. *Int. J. Appl. Earth Observ. Geoinf.* **2003**, 217–229. [CrossRef]

74. Baatz, M.; Schäpe, A. Multiresolution Segmentation: An Optimization Approach for High Quality Multiscale Image Segmentation. In *Angewandte Geographische Informationsverarbeitung*; Wichmann Verlag: Karlsruhe, Germany, 2000; pp. 12–23.

75. Marmanis, D.; Wegner, J.D.; Galliani, S.; Schindler, K.; Datcu, M.; Stilla, U. Semantic Segmentation of Aerial Images with an Ensemble of CNNs. *ISPRS Ann. Photogramm. Remote Sens. Spat. Inf. Sci.* **2016**, *3*, 473–480. [CrossRef]

76. Sherrah, J. Fully Convolutional Networks for Dense Semantic Labelling of High-Resolution Aerial Imagery. *arXiv* **2016**, arXiv:1606.02585.

77. Fu, G.; Liu, C.; Zhou, R.; Sun, T.; Zhang, Q. Classification for High Resolution Remote Sensing Imagery Using a Fully Convolu-tional Network. *Remote Sens.* **2017**, *9*, 498. [CrossRef]

78. Nguyen, T.; Han, J.; Park, D.-C. Satellite image classification using convolutional learning. In Proceedings of the 11th International Conference of Numerical Analysis and Applied Mathematics 2013, Rhodes, Greece, 21–27 September 2011; AIP Publishing: Melville, NY, USA, 2013; pp. 2237–2240.

79. Castelluccio, M.; Poggi, G.; Sansone, C.; Verdoliva, L. Land use classification in remote sensing images by convolutional neural networks. *arXiv* **2015**, arXiv:1508.00092.

80. Xue, G.; Liu, S.; Ma, Y. A hybrid deep learning-based fruit classification using attention model and convolution autoencoder. *Complex Intell. Syst.* **2020**, 1–11. [CrossRef]

81. Jozdani, S.E.; Johnson, B.A.; Chen, D. Comparing Deep Neural Networks, Ensemble Classifiers, and Support Vector Machine Algorithms for Object-Based Urban Land Use/Land Cover Classification. *Remote Sens.* **2019**, *11*, 1713. [CrossRef]

82. Ullah, F.; Sepasgozer, S.; Tahmasebinia, F.; Sepasgozar, S.M.E.; Davis, S. Examining the impact of students' attendance, sketching, visualization, and tutors experience on students' performance: A case of building structures course in construction management. *Constr. Econ. Build.* **2020**, *20*, 3. [CrossRef]

83. Ahmad, K.; Pogorelov, K.; Riegler, M.; Ostroukhova, O.; Halvorsen, P.; Conci, N.; Dahyot, R. Automatic detection of passable roads after floods in remote sensed and social media data. *Signal Process. Image Commun.* **2019**, *74*, 110–118. [CrossRef]

84. Shabir, O. A Summary Case Report on the Health Impacts and Response to the Pakistan Floods of 2010. *PLoS Curr.* **2013**, *5*, 5. [CrossRef]

85. Cengil, E.; Cinar, A.; Ozbay, E. Image classification with caffe deep learning framework. In Proceedings of the 2017 International Conference on Computer Science and Engineering (UBMK), Antalya, Turkey, 5–8 October 2017; Institute of Electrical and Electronics Engineers (IEEE): Piscataway, NJ, USA, 2017; pp. 440–444.

86. Georgakopoulos, S.V.; Tasoulis, S.K.; Vrahatis, A.G.; Plagianakos, V.P. Convolutional Neural Networks for Toxic Comment Classification. In Proceedings of the 10th Hellenic Conference on Artificial Intelligence, Patras, Greece, 9–12 July 2018; ACM: New York, NY, USA, 2018; p. 35.

87. Ahmad, K.; Pogorelov, K.; Riegler, M.; Conci, N.; Halvorsen, P. Social media and satellites: Disaster event detection, linking and summarization. *Multimed. Tools Appl.* **2019**, *78*, 2837–2875. [CrossRef]